Stem Cell Reports, Volume *5*

Supplemental Information

Dynamics of *Lgr6*$^+$ Progenitor Cells in the Hair Follicle, Sebaceous Gland, and Interfollicular Epidermis

Anja Füllgrabe, Simon Joost, Alexandra Are, Tina Jacob, Unnikrishnan Sivan, Andrea Haegebarth, Sten Linnarsson, Benjamin D. Simons, Hans Clevers, Rune Toftgård, and Maria Kasper

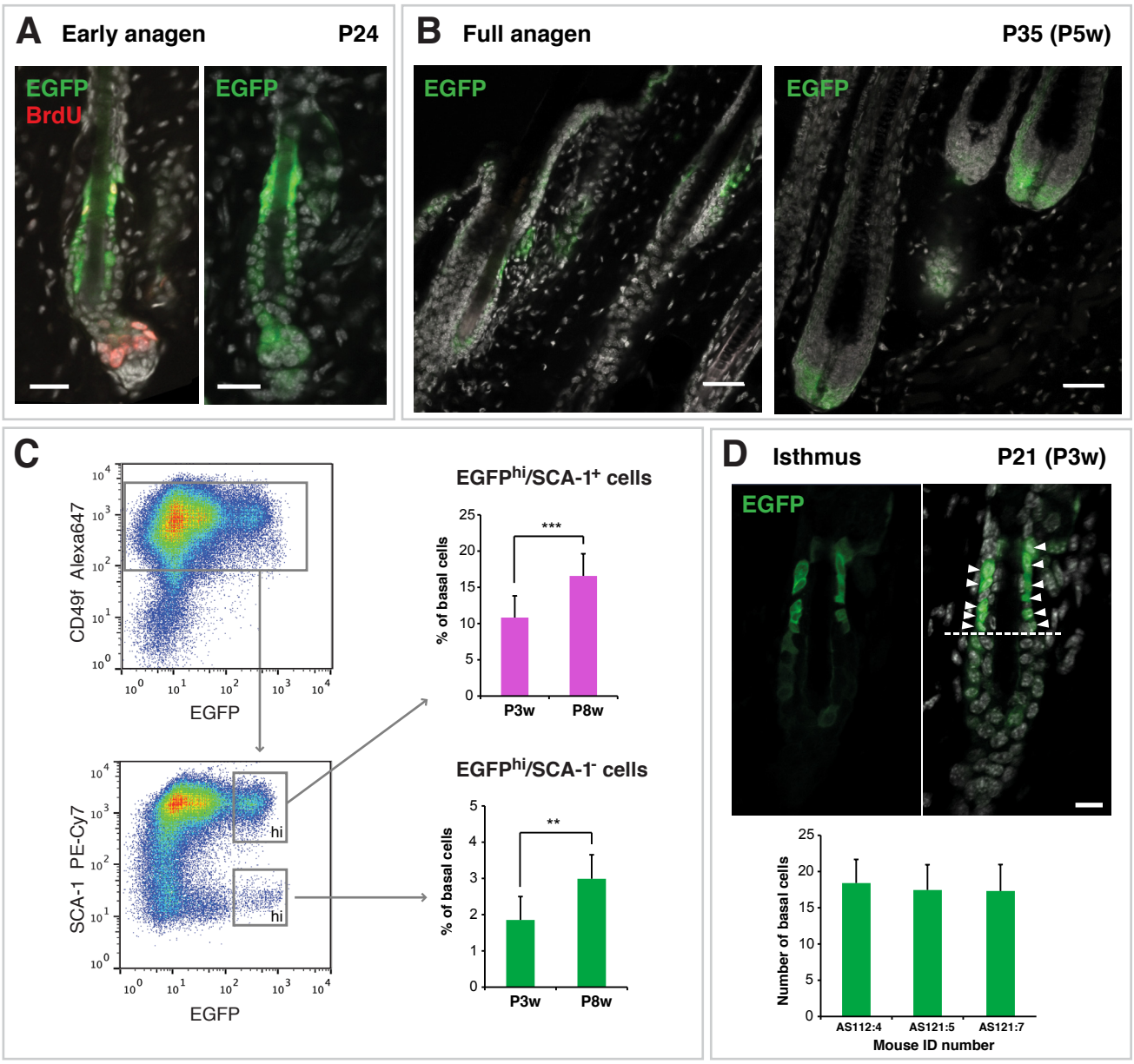
A
Early anagen
P24
EGFP
BrdU
EGFP
B
Full anagen
P35 (P5w)
EGFP
EGFP
C
CD49f Alexa647
EGFP
SCA-1 PE-Cy7
EGFP
hi
hi
EGFP^hi/SCA-1+ cells
% of basal cells
***
P3w
P8w
EGFP^hi/SCA-1- cells
% of basal cells
**
P3w
P8w
D
Isthmus
P21 (P3w)
EGFP
Number of basal cells
AS112:4
AS121:5
AS121:7
Mouse ID number

Figure S1

Figure S1. *Lgr6* expression during anagen and quantification of *Lgr6*$^{+}$ cells, related to Figure 1.

(A) Staining in skin of *Lgr6-EGFP-Ires-CreERT2* mice with anti-EGFP and anti-BrdU after a 2-hour BrdU pulse at the early anagen stage displays BrdU incorporation and EGFP expression in the expanding hair germ (n = 3 mice). Staining with anti-EGFP/anti-BrdU (left panel) and anti-EGFP only (right panel) are shown because BrdU-staining pretreatment lowers the anti-EGFP signal.
(B) EGFP antibody staining in skin of *Lgr6-EGFP-Ires-CreERT2* mice in anagen exhibits EGFP expression at the same sites as in telogen skin in the upper part of the PSU (left panel) and additional EGFP expression in the proximal anagen HF (right panel) (n = 3 mice).
(C) FACS quantification of EGFP expressing cells. Keratinocytes were isolated from skin of *Lgr6-EGFP-Ires-CreERT2* mice at P3w or P8w and stained with anti-CD49f and anti-SCA-1 antibodies to select for basal cells (CD49f^{+}) and discriminate IFE cells (SCA-1^{+}). The percentage of EGFP^{hi} cells was determined in the SCA-1^{+} and SCA-1^{-} basal fraction (P3w: n = 11 mice; P8w: n = 7 mice).
(D) Quantification of *Lgr6*^{IST} cells per PSU in P3w telogen skin. EGFP-antibody stained isthmus cells in skin of *Lgr6-EGFP-Ires-CreERT2* mice were counted in consecutive z-planes covering the entire isthmus in diameter (n = 3 mice; ≥ 7 entire HFs per mouse). Dashed line marks the bulge-isthmus border and arrowheads indicate the EGFP-expressing isthmus cells considered for *Lgr6*^{IST} quantification.
TO-PRO-3 nuclear stain (A, B and D). Scale bars, 25 μm (A), 50 μm (B), 10 μm (D).

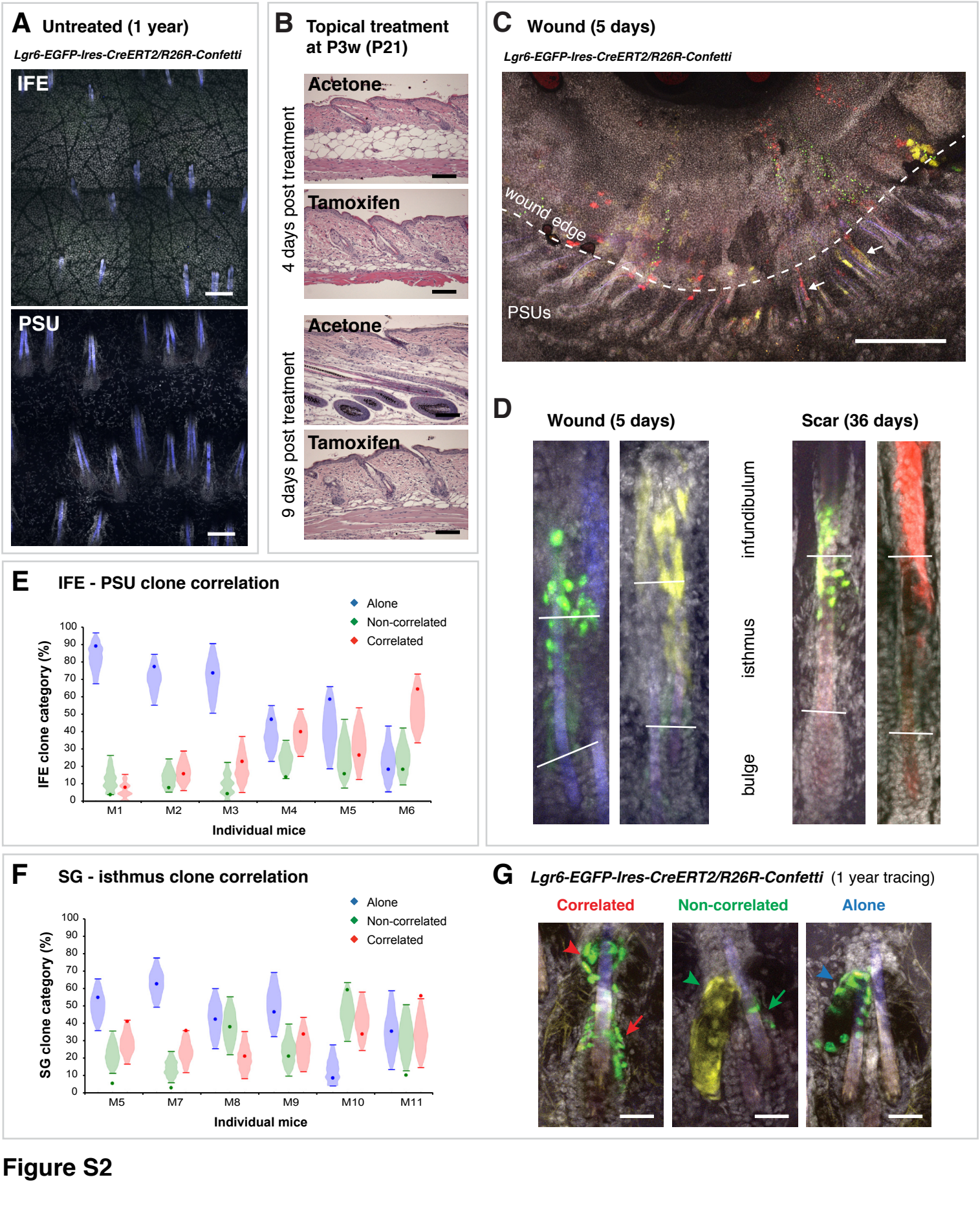
A Untreated (1 year)
Lgr6-EGFP-Ires-CreERT2/R26R-Confetti
IFE
PSU
B Topical treatment at P3w (P21)
4 days post treatment
Acetone
Tamoxifen
9 days post treatment
Acetone
Tamoxifen
C Wound (5 days)
Lgr6-EGFP-Ires-CreERT2/R26R-Confetti
wound edge
PSUs
D
Wound (5 days)
Scar (36 days)
infundibulum
isthmus
bulge
E IFE - PSU clone correlation
Alone
Non-correlated
Correlated
IFE clone category (%)
100
90
80
70
60
50
40
30
20
10
0
M1
M2
M3
M4
M5
M6
Individual mice
F SG - isthmus clone correlation
Alone
Non-correlated
Correlated
SG clone category (%)
100
90
80
70
60
50
40
30
20
10
0
M5
M7
M8
M9
M10
M11
Individual mice
G Lgr6-EGFP-Ires-CreERT2/R26R-Confetti (1 year tracing)
Correlated
Non-correlated
Alone

Figure S2

Figure S2. *Lgr6-EGFP-Ires-CreERT2/R26R-Confetti* lineage tracing during wound healing, and clone correlation between IFE-PSU and SG-IST, related to Figure 2.

(A) Representative z-stack projections of IFE and PSUs from a non-treated *Lgr6-EGFP-Ires-CreERT2/R26R-Confetti* mouse aged one year, demonstrating complete absence of labeling without tamoxifen (n = 3 mice). Hair shafts show autofluorescence in the blue channel.
(B) Hematoxylin/eosin stained sections from skin of *Lgr6-EGFP-Ires-CreERT2/R26R-Confetti* mice 4 and 9 days after topical treatment with tamoxifen or vehicle (acetone) at P3w. Tamoxifen-treated skin shows a delay in anagen induction compared to control skin (n = 3 mice).
(C) Representative whole mount image of a wound edge at day 5 after wounding in a *Lgr6-EGFP-Ires-CreERT2/R26R-Confetti* mouse treated with tamoxifen at P3w and wounded 4 days later (n = 3 mice). Arrows indicate the PSU clones contributing to IFE during wound closure.
(D) Representative confocal projections of $Lgr6^{PSU}$-traced clones in wound and scar environments in the dorsal skin demonstrate the survival of $Lgr6^{+}$ progeny in the infundibulum after wounding. Tamoxifen was given at P3w, wounds were made 4 days later, the wound tissue was analyzed 5 days after wounding (left panels, n = 3 mice), and the scar tissue was analyzed 36 days after wounding (right panels, n = 3 mice). Lines indicate the approximate borders between bulge, isthmus and infundibulum, and have a scale of 40 µm.
(E) Observed and expected percentages of "correlated", "non-correlated" and "alone" IFE clones compared to PSU clones. The observed percentages of each clone category are represented as dots. The expected percentages were estimated using a bootstrapping strategy assuming that IFE and PSU clones are not related (see Supplemental Experimental Procedures). The violin plots show the 95% confidence intervals of the expected percentages for each clone category and mouse. Note, in all mice and categories (18 out of 18), the observed values lay within the expected distribution, which implies that the IFE and the PSU clones are independent. The same mice and observed clone-categories as shown in Figure 2D and 2E were used. In total, 186 IFE clones and 875 PSUs were analyzed in 6 mice, which were traced for ≥40 days.
(F) Observed and expected percentages of "correlated", "non-correlated" and "alone" SG clones compared to isthmus clones. SG clones were assigned as shown in (G). The observed percentages of each clone category are represented as dots. The expected percentages were estimated using a bootstrapping strategy assuming that SG and isthmus clones are not related (see Supplemental Experimental Procedures). The violin plots show the 95% confidence intervals of the expected percentages for each clone category and mouse. Most of the observed values (14 out of 18) lay within the expected distribution, which is suggestive for independent compartment maintenance of isthmus and SG; however, a minor cellular exchange cannot be ruled out. In total, 165 SG clones were analyzed in 6 mice, which were traced for ≥40 days.
(G) Illustrative pictures of *Lgr6-EGFP-Ires-CreERT2/R26R-Confetti* mouse skin that was traced for 1 year showing SG clones that are isthmus-correlated (red arrowhead), non-correlated (green arrowhead) or alone (blue arrowhead).
Confetti clone colors in nuclear green, yellow, red and membranous blue (A, C, D and G), TO-PRO-3 nuclear stain in gray (A and C, D and G). Scale bars, 100 µm (A and B), 500 µm (C), 40 µm (D), 25 µm (G).

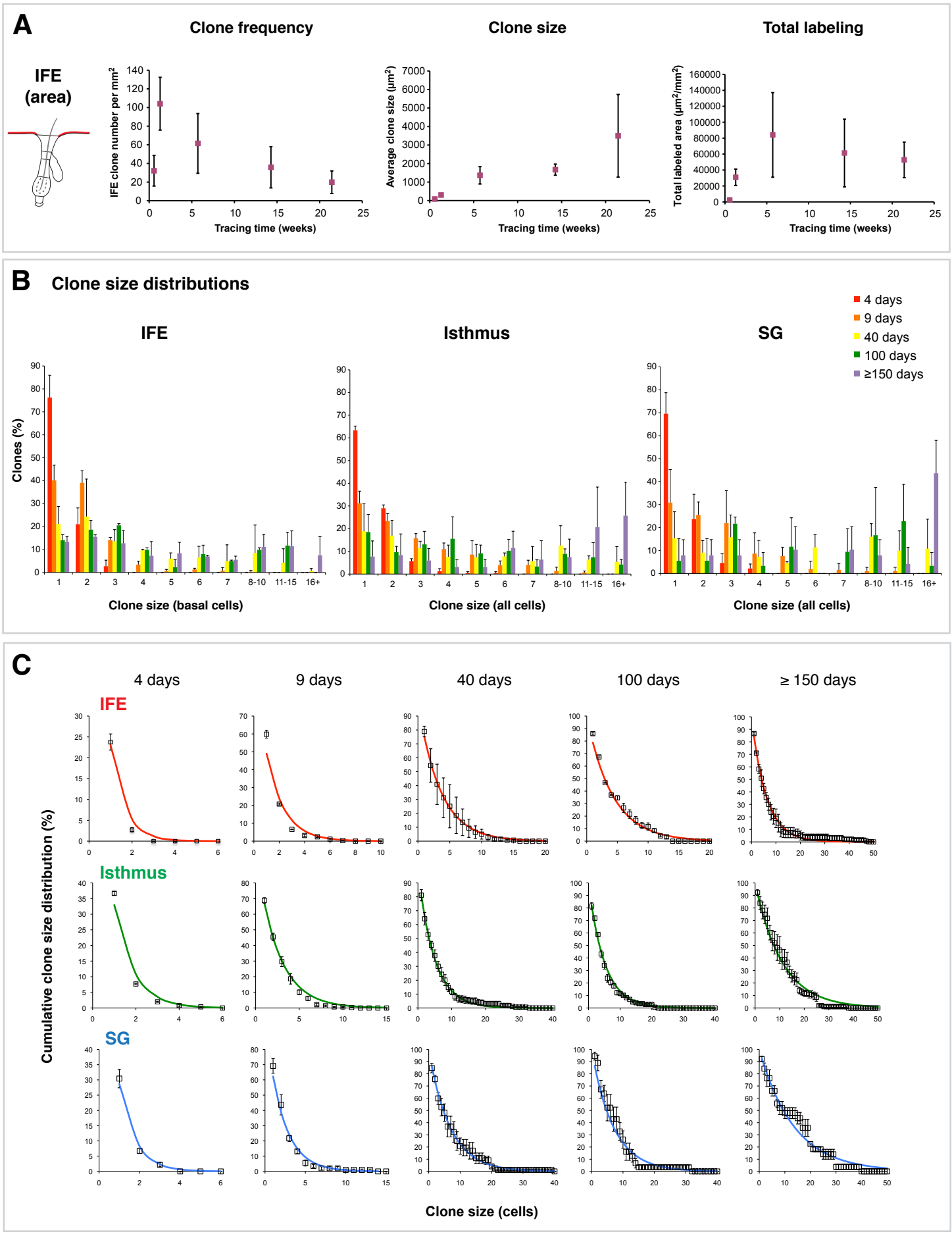
A
Clone frequency
Clone size
Total labeling
IFE (area)
IFE clone number per mm²
Average clone size (µm²)
Total labeled area (µm²/mm²)
Tracing time (weeks)
B
Clone size distributions
IFE
Isthmus
SG
4 days
9 days
40 days
100 days
≥150 days
Clones (%)
Clone size (basal cells)
Clone size (all cells)
C
4 days
9 days
40 days
100 days
≥ 150 days
IFE
Isthmus
SG
Cumulative clone size distribution (%)
Clone size (cells)

Figure S3

Figure S3. *Lgr6*$^+$ clone dynamics and clone size distributions, related to Figure 3.

(A) *Lgr6-EGFP-Ires-CreERT2/R26R-Confetti* clone dynamics in the IFE was additionally measured by determining the total area of the clones in z-stack projections of flat-mount images. The average IFE clone number is higher than in the basal-cell clone analysis due to inclusion of clones without basal cells. Similar dynamics of decreasing clone frequency and increasing clone size were confirmed. The total labeled area reached the highest level only after 5.5 weeks tracing as the clones of earlier time points consisted mostly of basal cells.
(B) Histograms displaying the percentage of clones of different sizes (numbers of cells) in IFE, isthmus and SG. The clone size distributions become broader with time.
(C) Cumulative clone size distributions in IFE, isthmus and SG show an exponential shape matching the predictions of the committed progenitor model. At clone size n, the chance of finding a surviving *Lgr6*$^+$-derived clone with more than n cells is shown.
Data are shown as mean of 3 mice ± SD (A and B) or ± SEM (C).

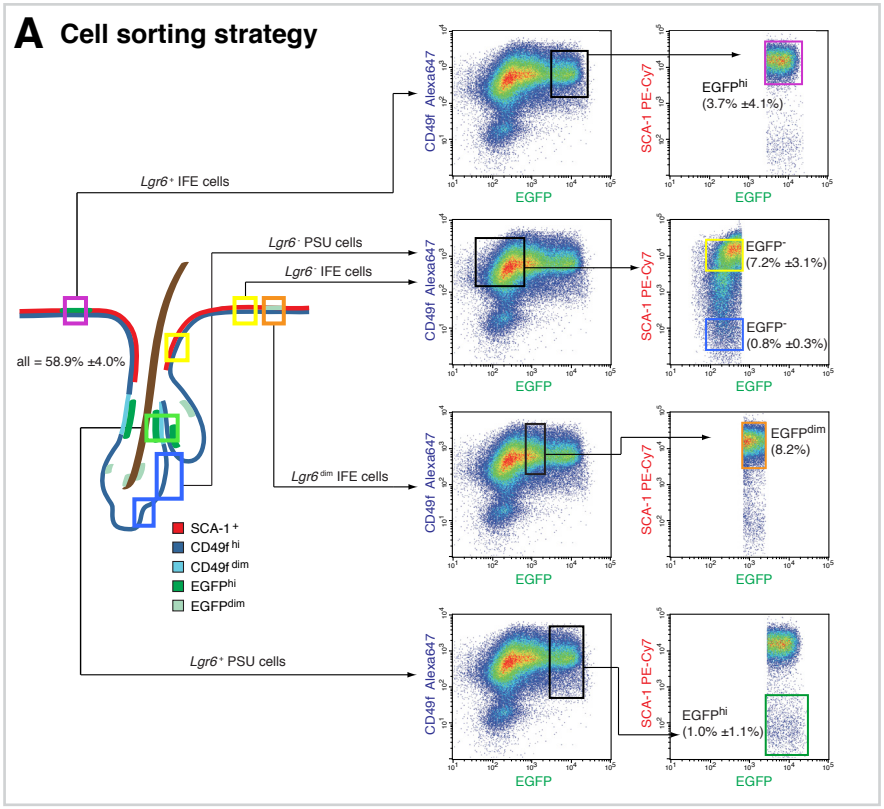
A Cell sorting strategy
Lgr6+ IFE cells
Lgr6- PSU cells
Lgr6- IFE cells
Lgr6dim IFE cells
Lgr6+ PSU cells
all = 58.9% ±4.0%
SCA-1+
CD49fhi
CD49fdim
EGFPhi
EGFPdim
CD49f Alexa647
SCA-1 PE-Cy7
EGFP
EGFPhi (3.7% ±4.1%)
EGFP- (7.2% ±3.1%)
EGFP- (0.8% ±0.3%)
EGFPdim (8.2%)
EGFPhi (1.0% ±1.1%)

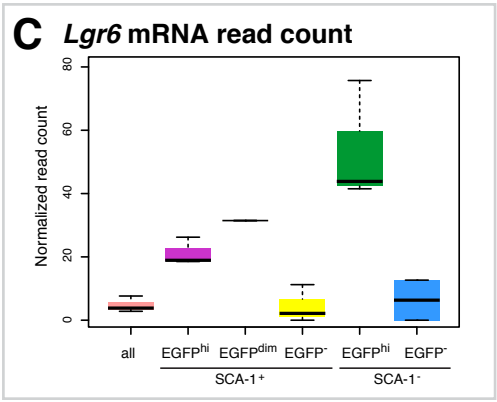
C Lgr6 mRNA read count
Normalized read count
all
EGFPhi
EGFPdim
EGFP-
EGFPhi
EGFP-
SCA-1+
SCA-1-

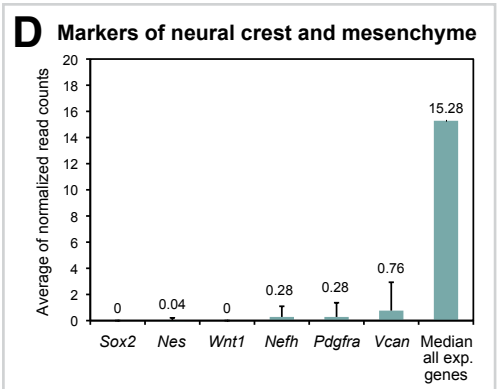
D Markers of neural crest and mesenchyme
Average of normalized read counts
0
0.04
0
0.28
0.28
0.76
15.28
Sox2
Nes
Wnt1
Nefh
Pdgfra
Vcan
Median all exp. genes

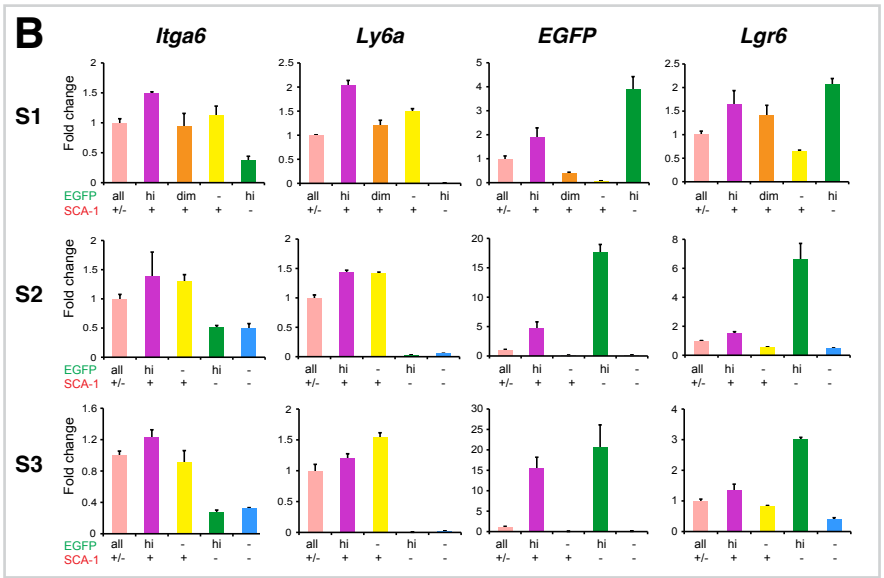
B
Itga6
Ly6a
EGFP
Lgr6
S1
S2
S3
Fold change
EGFP
SCA-1
all
hi
dim
-

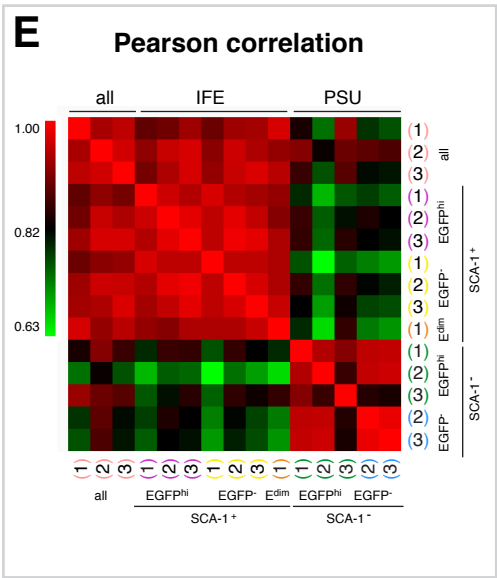
E Pearson correlation
all
IFE
PSU
1.00
0.82
0.63
EGFPhi
EGFP-
Edim
SCA-1+
SCA-1-

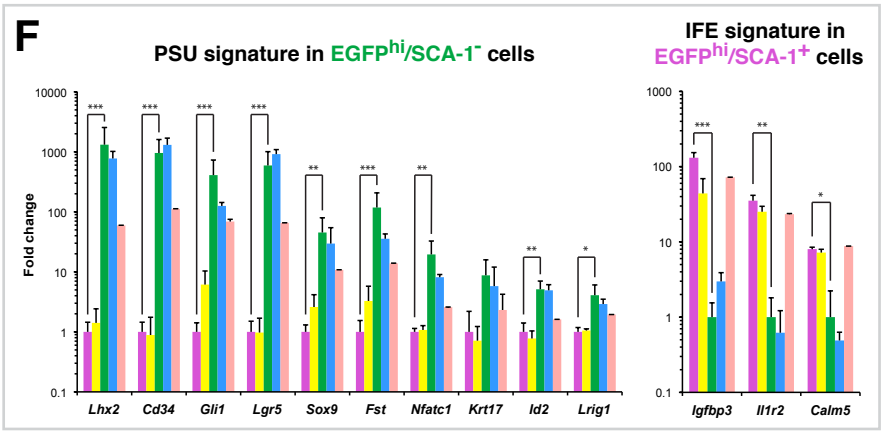
F
PSU signature in EGFPhi/SCA-1- cells
IFE signature in EGFPhi/SCA-1+ cells
Fold change
Lhx2
Cd34
Gli1
Lgr5
Sox9
Fst
Nfatc1
Krt17
Id2
Lrig1
Igfbp3
Il1r2
Calm5

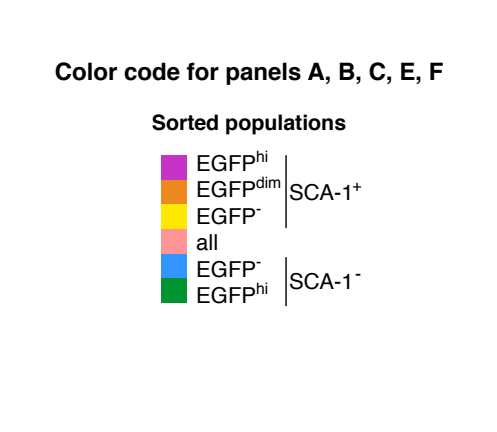
Color code for panels A, B, C, E, F
Sorted populations
EGFPhi
EGFPdim
EGFP-
all
EGFP-
EGFPhi
SCA-1+
SCA-1-

Figure S4

Figure S4. RNA-seq analysis of FACS-sorted *Lgr6*$^{+}$ and *Lgr6*$^{-}$ keratinocyte populations, related to Figure 4.

(A) Scheme illustrating the sorting strategy for the different keratinocyte populations used for RNA-seq analysis, including illustrative FACS plots of all sorted keratinocyte populations. The size of the populations is represented as a percentage of all measured (ungated) cells ± SD.
(B) Real-time PCR analysis of the sorting markers CD49f (*Itga6*), SCA-1 (*Ly6a*) and EGFP was used to validate the purity of the populations in each sorting (S1–S3), and *Lgr6* expression was measured to display the relative levels of *Lgr6* and *EGFP* mRNA expression in the respective sorted samples. Data are shown as mean of three technical replicates (± SD) assayed in each of the three independent sortings.
(C) Boxplots showing normalized *Lgr6* mRNA reads in the different populations, measured by RNA-seq and normalized using DESeq, which confirms that the *Lgr6* mRNA levels were in agreement with EGFP protein levels.
(D) Mean normalized RNA-seq read counts (of all sorted samples) of genes associated with mesenchymal or neural origin. For comparison, the median read count of all expressed genes (read count >0) is presented. The absence or very low read counts for these marker genes ruled out contamination of the sorted populations by non-epithelial cells.
(E) Heatmap showing Pearson correlations across all genes, pairwise for all samples from the three independent cell sortings.
(F) Real-time PCR analysis of selected genes that represent the transcriptional PSU- or IFE-phenotype of EGFP^{hi}/SCA-1^{-} and EGFP^{hi}/SCA-1^{+} cells, respectively. Data are shown as mean of ≥ 2 biological replicates ± SD. Significance tests were performed between EGFP^{hi}/SCA-1^{-} and EGFP^{hi}/SCA-1^{+} populations (n = 3 biological replicates). Asterisks indicate T-test significance level at $p<0.05$ (*), $p<0.01$ (**) and $p<0.001$ (***).

SUPPLEMENTAL TABLES

Table S1. Comparison of the observed with the expected frequencies of Confetti-clone colors in IFE and PSU, related to Figure 2.

Mouse ID	AS30:5 (M4)	AS30:7 (M3)	AS42:3 (M6)	AS55:2 (M5)	AS51:4 (M2)	AS55:3 (M1)
Correlated $_{observed}$	0.395	0.227	0.636	0.263	0.158	0.080
μ (Correlated $_{simulated}$)	0.333	0.197	0.552	0.373	0.180	0.065
2σ (Correlated $_{simulated}$)	0.169	0.143	0.178	0.174	0.137	0.088
Non correlated $_{observed}$	0.140	0.0455	0.182	0.158	0.079	0.040
μ (Non correlated $_{simulated}$)	0.220	0.157	0.243	0.231	0.146	0.061
2σ (Non correlated $_{simulated}$)	0.149	0.131	0.154	0.151	0.127	0.086
No label $_{observed}$	0.465	0.727	0.182	0.579	0.763	0.880
μ (No label $_{simulated}$)	0.447	0.646	0.204	0.397	0.674	0.874
2σ (No label $_{simulated}$)	0.179	0.172	0.145	0.176	0.168	0.119

Table S2. *Lgr6-EGFP-Ires-CreERT2/R26R-Confetti* mice and clones evaluated for each time point, related to Figure 3.

	4 days					9 days				40 days			100 days			≥ 150 days			
Mouse ID (AS no.)	42:1	42:6	45:2	48:2	48:3	42:6	45:2	48:2	157:1	51:1	90:7	152:7	42:2	51:2	122:3	42:1	51:4	90:4	122:6
Days traced	4	4	4	4	4	9	9	9	9	40	41	39	99	103	101	143	194	160	149
HFs counted	NA	NA	73	110	92	NA	76	70	57	98	85	101	94	73	52	100	179	65	NA
Total HF clones	NA	NA	81	121	114	NA	140	136	87	109	76	153	76	21	71	56	14	53	NA
Total labeled HF cells	NA	NA	109	179	164	NA	399	367	213	742	258	723	498	114	308	394	173	441	NA
Isthmus clones	NA	NA	43	88	74	NA	95	89	56	54	38	97	54	15	45	38	5	30	NA
Total labeled isthmus cells	NA	NA	62	134	108	NA	308	259	133	431	154	453	320	72	227	260	75	319	NA
SG clones	NA	NA	25	27	35	NA	25	34	21	27	21	20	10	5	12	8	5	9	NA
Total labeled SG cells	NA	NA	32	39	51	NA	47	91	59	192	58	188	86	33	46	93	77	101	NA
IFE clones	32	27	62	17	68	110	144	141	NA	90	290	91	80	23	82	72	66	75	32
IFE basal clones	32	27	62	17	66	84	104	118	NA	64	NA	70	65	20	NA	60	NA	68	32
Total labeled IFE cells	36	31	81	24	88	173	205	212	NA	158	NA	375	291	101	NA	296	NA	610	572
HF clone color distribution																			
Blue (%)	NA	NA	1.2	0.0	3.5	NA	6.4	11.8	37.9	0.0	21.1	11.8	0.0	0.0	15.5	0.0	0.0	11.3	NA
Green (%)	NA	NA	6.2	1.7	6.1	NA	9.3	20.6	29.9	15.6	0.0	32.0	2.6	0.0	28.2	0.0	7.1	3.8	NA
Yellow (%)	NA	NA	42.0	48.3	45.6	NA	40.7	33.1	28.7	35.9	40.8	29.4	46.8	52.4	29.6	53.6	50.0	34.0	NA
Red (%)	NA	NA	50.6	50.0	44.7	NA	45.7	33.8	3.4	48.4	38.2	28.1	50.6	47.6	26.8	46.4	42.9	50.9	NA

Table S3. Primers for cDNA amplification, related to Figures 4 and S4.

The primers were optimized for the following conditions: 5 min at 94 °C initial denaturation, 10 cycles of [1 min at 94 °C denaturation, 1 min at 60 °C annealing, and 2 min at 72 °C extension].

Gene	Forward primer sequence 5'-3'	Reverse primer sequence 5'-3'
Alcam	TTGTGGGAATTGTCGTTGGTCT	CAATCCACGTTCATGCTTCAAT
Calm5	AATGAAGCAGTTGGGCAAGAAC	CAAAAACTGCTCATAGTTCACCTTCC
Cd34	CCACTTCAGAGATGACCTGGAA	GGCTAGAAGCAGGGAGCAGA
Cd44	GAACAGGACAGGACCACTTTCA	CCTGGTAAGGAGCCATCAACAT
Cst6	TAGAAAGCACAGAGTGCCGAAA	AGGAGAAAGCAGTGCAAGAAGC
Defb6	CCTGCTCTTTGCCTTTATCCTG	GATTTTAGGATGGCCACAATGGC
EGFP	ATGGCCGACAAGCAGAAGAA	GTCCATGCCGAGAGTGATCC
Fst	GGAAAACCTACCGCAACGAAT	TTCAGAAGAGGAGGGCTCTGG
Fzd1	CTCGCCAGCCACTGACTTTT	GCAGAAAAGGGCAAGTGAGAAA
Gli1	GCCGCCTGGAGAACCTTAG	GGTAGTGACGATGCCCCATT
Hprt1	GGGGGCTATAAGTTCTTTGC	TCCAACACTTCGAGAGGTCC
Id2	GACCCGATGAGTCTGCTCTAC	TTCGACATAAGCTCAGAAGGGAAT
Igfbp3	TCAAAGCACAGACACCCAGAAC	CACGGAGCATCTACTGGCTCT
Il1r2	ATACCAGCATCATTGGGGTCA	TCCAGGAGAACGTGGAAGAGA
Itga6	TCAGGAGTAGCTTGGTGGATCA	CGAGGTTATCCATGTGTTTCTCA
Krt14	CACCATGCAGAACCTGGAGAT	TGGATGACTGAGAGCCAGAGG
Krt17	GCAGAACCAGGAGTACAAGATCC	GCTGTAGCAGGAGGGTGATG
Lgr5	CCGAGCCTTACAGAGCCTGA	AGGTGCTCACAGGGCTTGAA
Lgr6	TCAGGGAACCACCTCTCACAC	TGGAAGGCATAGTCAGGGATG
Lhx2	GTCTATTGCCGCTTGCACTTC	GTCTTTTGGCTGCTGGGGTAG
Lrig1	GGTCCCTCTATCCAAGCAACC	TCCCAGTGATCTGCCCTTTC
Ly6a	CTCAGGGACTGGAGTGTTACC	GCAGAGGTCTTCCTGGCAAC
Nfatc1	AGCCCCGTCCAAGTCAGTTT	GCAGGAGAGGAAAGGTCGTG
Nrp1	CAACTGGTCTGGATGGTGGTT	TAAGCACATTGCCTGGCTTC
Pthlh	GGTTTGAGAGAGGCGCAGTT	TCTGATTTCGGCTGTGTGGA
Rplp0	CCTGAAGTGCTCGACATCACA	CCTCCGACTCTTCCTTTGCT
Sostdc1	TCCTCCTGCCATTCATCTCTC	CATAGCCTCCTCCGATCCAGT
Sox4	TGCCTCATGGTCAAGAAAGGA	GCTACTCCCAGCACATCTCCA
Sox9	AGGTGCTGAAGGGCTACGACT	CCGGGGCTGGTACTTGTAATC
Tcf7l2	AACCCTCAAGGATGCTCGTTC	TCCTCCTGTCGTGATTGGGTA
Tnfrsf19	CAATGTATGGGCCTGTTCACCT	CGGGATTGAGGGAATTGGTATC
Wnt6	CTCCAGGACCAACTGGCTCTC	AGAGCTTTGCCGTCGTTGGTG

Table S4. Primers for qPCR, related to Figures 4 and S4.

The primers were optimized for the following conditions: 3 min at 95 °C initial denaturation, 42 cycles of [15 s at 95 °C denaturation, 15 s at 65 °C annealing, and 30 s at 72 °C extension].

Gene	Forward primer sequence 5'-3'	Reverse primer sequence 5'-3'
Alcam	CCTCGTTGCTGGTGTCGTCTACTGG	CAGGCTATCCAATCCGCTCCTCTCT
Calm5	GCAGGCTATGTTCAGTGTCCTTGACC	TTCACCTTCCCATCTTGGTCTGCAC
Cd34	GATGACATCACCCACCGAGCCATA	CCTCAGCCTCCTCCTTTTCACACAG
Cd44	GGAGAGCCGGAAGAAGACGAAAACC	AGCAGGGGTCACTGGGAAGAGAGTC
Cst6	ACATGGACCTCACCACCTGCCCTCT	GCTGAGTAGTGTTCTTCCAGGGGACTTCA
Defb6	ATCTCTGCACCTCACCAGGCATCAG	GCTGTCTCCACTTGCAGCCTTTTCC
EGFP	GATCCGCCACAACATCGAGGACG	GGCGGTCACGAACTCCAGCAG
Fst	GCACTCCTCAAGGCCAGATGCAAAG	CACAAGTGGAGCTGCCTGGACAAAA
Fzd1	CCCTTTCCCAACAAACAGCACAGGT	AGATCGGTCCACACGCACATACACA
Gli1	CCCATAGGGTCTCGGGGTCTCAAAC	GGAGGACCTGCGGCTGACTGTGTAA
Hprt1	CAACGGGGGACATAAAAGTTATTGGTGG	TGCAACCTTAACCATTTTGGGGCTGT
Id2	GGACTCGCATCCCACTATCGTCAGC	GGGAATTCAGATGCCTGCAAGGACAG
Igfbp3	AGGCGTCCACATCCCAAACTGTGAC	TCGTCTTTCCCCTTGGTGTCGTAGC
Il1r2	TGACCGAGGGGCTACACCACCAGTA	CTCCGTGGATTCGAGGCAACACATT
Itga6	CTGTTCTTGCCGGGATTCTGATGCT	GCATGGTATCGGGGAATGCTGTCAT
Krt14	TGCTGGATGTGAAGACAAGGCTGGA	GGAAGATGAAAGGTGGGCGTCCTCT
Krt17	AAGACAAGGCTGGAGCAGGAGATCG	GCTGAGTCCTTAACGGGTGGTCTGG
Lgr5	CCAATGGAATAAAGACGACGGCAACA	GGGCCTTCAGGTCTTCCTCAAAGTCA
Lgr6	CTGGACCCCCTGACGGCTTACCT	GATCCCACGGAGCTGGTTGCTCT
Lhx2	CCTACTACAACGGCGTGGGCACTGT	GTCACGATCCAGGTGTTCAGCATCG
Lrig1	GCAGATGGGAACGGAGATTCCTCTTG	TGCTGGGCTTCAGTAGATATGGCGTC
Ly6a	TGCCCCTACCCTGATGGAGTCTGTG	GGAGGGCAGATGGGTAAGCAAAGATTG
Nfatc1	ATGTCTGCAACGGGAAACGGAAGAG	AGGCATGGTGAGCTGTTGGCTGTAG
Nrp1	GGAAACCTTGGTGGAATTGCTGTGG	TCTTGTCACCTTCCCCTTCTCCTTCA
Pthlh	TGGTTCAGCAGTGGAGTGTCCTGGT	GATGGACTTGCCCTTGTCATGCAGT
Rplp0	TGCACTCTCGCTTTCTGGAGGGTGT	AATGCAGATGGATCAGCCAGGAAGG
Sostdc1	CCAGCAGCAACAGCACCCTGAATC	TGCACTGGCCGTCCGAAATGTAT
Sox4	CCATCTCCTACCCACCCCCTCTTTG	TTCTCCATGCCAATGCTCCCCTAAG
Sox9	CAGACCAGTACCCGCATCTGCACAA	AAGGGTCTCTTCTCGCTCTCGTTCAGC
Tcf7l2	TCACGCCTCTCATCACGTACAGCAA	CCTAGCGGATGGGGGATTTGTCCTA
Tnfrst19	GATTCCGTCCTTGTGCTGTGAAGAGG	GGAACGGGAAACAGACCCGAAGAAG
Wnt6	AGGCTGCGGAGACGATGTGGACTT	GCAGAGCGCAGGAACCCGAAAG

SUPPLEMENTAL EXPERIMENTAL PROCEDURES

Microscopy and image analysis

Imaging was performed using an LSM710-NLO confocal microscope (Zeiss) or a Nikon A1R confocal microscope. Confetti-color detection was carried out on the Zeiss microscope using 405-nm, 488-nm, 514-nm and 561-nm lasers for CFP, GFP, YFP and RFP/TO-PRO-3, respectively, and images were acquired with a 20x water-dipping objective at 1024x1024 resolution. Combinations of z-stack and tiling images were recorded using narrow filtering on spectral detectors to avoid bleed-through. Z-stack images of RNA *in situ* stainings were recorded with a z-distance of 0.65 µm using a 60x objective. Image analysis was performed using NIS-Elements software (Nikon), Zen 2009 software (Zeiss), or ImageJ, and images were occasionally optimized for brightness, contrast, and color balance.

Horizontal whole mount (HWM) IF staining

Samples of dorsal skin were fixed in 4% PFA for 20 min and mounted in OCT embedding medium (Histolab). Subsequently, 150-µm sections were cut with a cryostat, blocked with PB buffer (0.1% fish skin gelatin, 0.5% Triton X-100 and 0.5% skimmed milk powder in PBS) and stained as described previously (Driskell et al., 2009). The nuclear stain, TO-PRO-3 (Invitrogen, 1:1000), was applied at the same time as secondary antibodies (Alexa Fluor Dyes 488, 546, 647 or 680; Invitrogen, 1:500).

RNA *in situ* hybridization (ISH) on paraffin sections

ISH was performed on PFA-fixed and paraffin-embedded skin sections using the RNAscope Fluorescent Multiplex Kit (Advanced Cell Diagnostics, Inc.) according to the manufacturer's instructions. Critically, skin tissue sections were heat-pretreated for 15 min and underwent protease digestion for 30 min. The following RNAscope probes were used: *Lgr6* (ACD404961), *Defb6* (ACD430141) and *Krt5* (ACD415041). The housekeeping gene *Polr2a* served as a positive control whereas a probe targeting the bacterial mRNA *dapB* was used as a negative control on consecutive skin sections.

Real-time PCR

Real-time PCR was performed on the same RNA samples used for sequencing after pre-amplification of the cDNA with gene-specific, nested primers. Per sample, 2 ng RNA were reverse-transcribed using Superscript III First-Strand Synthesis Kit (Invitrogen) and gene-specific reverse primers for the outer nested PCR product. Then, gene-specific forward primers were added, and the cDNA was amplified for 10 cycles, generating the outer nested PCR products. The resulting amplified cDNA was analyzed with real-time PCR using a second pair gene-specific primers located within the sequence of the nested PCR fragment. The assays were run using Power SYBR Green PCR Master Mix on a 7900HT Fast Real-Time PCR system (both Applied Biosystems). All primers were designed to span exon boundaries using the Primer 3 online tool. Complete lists of primer sequences and PCR conditions are available in Tables S3 and S4.

Confetti clone definition and categorization

First, cohesively connected cells in the same color were defined as one clone. To place the cells within the distinct compartments of the PSU, we used anatomical features such as the SG-opening (demarcating the upper and lower border of the junctional zone), or the inner bulge cells to identify the lower border of the isthmus.

Figure 2. For the IFE – PSU correlation analysis, an IFE clone of a given color (e.g. red) was picked, and compared with every PSU surrounding the IFE clone in a radius of 150–200 µm. If there was at least one red clone in one of the surrounding PSUs, the IFE clone was categorized 'correlated'. If there was no red clone in these PSUs, but at least one clone in another color, the IFE clone was categorized 'non-correlated', and if none of the surrounding PSUs were labeled, the IFE clone was categorized 'alone'.
For the SG – isthmus correlation analysis, a SG clone of a given color (e.g. red) was picked, and compared with the lower isthmus of the same PSU. If there was at least one red clone in the lower isthmus (green area in Figure 2B), the SG clone was categorized as 'correlated'. If there was no red clone in the lower isthmus, but at least one clone in another color, the SG clone was categorized 'non-correlated', and if there was no clone in the lower isthmus, the SG clone was categorized 'alone'.
Figure 3. Isthmus clones were defined as having at least one cell in the lower isthmus (see Figure 2B, green area) and all cohesively connected cells of the same Confetti color were counted for quantification of the clone size. SG clones were defined as having at least one cell in the SG (see Figure 2B, blue area) and at the same time no connected cell of the same color in the lower isthmus area. All cohesively connected cells of the same Confetti color were used for SG clone size quantification.

Simulation strategy for IFE – PSU color correlation
The simulation analysis was performed using Python, and the scripts are available upon request. In order to simulate the expected IFE – PSU color correlation as a function of labeling efficiency (Figure 2E), under the assumption that IFE and PSU are independent compartments, we devised the following simulation model:

For each labeling efficiency ***L*** (from 0.05–1 in incremental steps of 0.05), we simulated 100.000 experiments. In each experiment, we assigned each of ***n_clones_IFE*** IFE clones with a color ***c_IFE***. We then chose a number of ***n_PSU*** surrounding PSUs for each IFE clone and subsequently determined the number of PSU clones ***n_clones_PSU*** in dependency of ***L*** for each PSU and the corresponding color ***c_PSU*** for each PSU clone. Next, we marked each IFE clone as 'correlated', 'non-correlated' or 'alone' depending on whether the surrounding PSUs carry a correlated clone, only uncorrelated clones or no clones at all. For each experiment, we return the fraction of IFE clones which were marked as 'correlated', 'non-correlated' or 'alone' and for each labeling efficiency, we return the mean and standard deviations of those values derived from 100.000 experiments.

The number ***n_clones_IFE*** of IFE clones simulated per experiment is based on the average number of IFE clones counted in each empirical experiment.

The number ***n_PSU*** of surrounding PSUs per IFE clone is randomly chosen from a Poisson distribution with a λ that reflects the average number of PSUs per IFE clone as observed over all empirical experiments. While the empirical distribution of HFs per IFE clone is slightly underdispersed compared to a Poisson distribution (data not shown), we regard it as a robust approximation.

The colors ***c_IFE*** and ***c_PSU*** for each IFE and PSU clone are randomly chosen based on the empirically determined color probabilities for IFE and PSU clones averaged over all empirical experiments.

We assumed that the number ***n_clones_PSU*** of clones per PSU – the most critical parameter in the simulation – could be derived from a discrete probability distribution in dependency of ***L***, which we define as average number of clones per PSU ***μ(n_clones_PSU)***. The empirical values for ***n_clones_PSU*** point to a distribution that is overdispersed compared to an ideal Poisson distribution (not shown). Such a distribution can be modeled as Gamma mixture of Poisson distributions. Hence

$n\_clones\_PSU \sim Poisson(\lambda) \qquad \lambda \sim Gamma(k, \theta)$

with

$\mu(n\_clones\_PSU) = L = k\,\theta \qquad \sigma(n\_clones\_PSU) = k\,\theta\,(1+\theta)$

We noted that in the empirical data, the variance ***σ(n_clones_PSU)*** scales linearly with the mean ***μ(n_clones_PSU***) = *L* and can thus be expressed as

$\sigma(n\_clones\_PSU) = r\,\mu(n\_clones\_PSU) = r\,L$

where ***r*** is an empirically determined dispersion factor. While a Gamma-Poisson mixture with $k = L / (r - 1)$ and $\theta = r - 1$ would perfectly model mean and variance of our empirical data, we noted that a Gamma-Poisson mixture with k = L / r and $\theta = r$ – while overstating the variance – provides an overall better fit to the empirically determined distribution of clones per PSU in dependency of *L*. We reason that the empirical distribution is truncated due to the limited space for clones in the isthmus and SG regions of the PSU and thus exhibits a lower variance compared to an ideal Gamma-Poisson distribution. We thus chose

$n_{IST} \sim Poisson(\lambda) \qquad \lambda \sim Gamma(L / r\,,\, r)$

as our final model.

Resampling strategy for IFE – PSU and SG – IST color correlation

As an alternative approach, we used bootstrapping methodology to infer the expected numbers of 'correlated', 'non-correlated' and 'alone' clones if **(a) IFE – PSU** and **(b) SG – IST** were independent compartments. In contrast to the simulation approach specified above, this resampling approach has the advantage that it does not rely on assumptions about the underlying distributions for each parameter but instead only uses the empirical data. The bootstrapping analysis was performed using Python, and the scripts are available upon request.

For each mouse analyzed in **(a) Figure S2E** and **(b) Figure S2F**, we extracted and employed following empirical data:

- **(a)** ***clones_per_IFE*** or **(b)** ***clones_per_SG*** (the number of IFE clones in all analyzed fields-of-view for **(a)** or the number of SG clones in all analyzed PSUs for **(b)**).

- **(a)** ***c_IFE*** or **(b)** ***c_SG*** (the number of B, G, Y, R clones among all IFE clones for **(a)** or the number of B (blue), G (green), Y (yellow), R (red) clones among all SG clones for **(b)**).

- **(a)** ***clones_PSU*** or **(b)** ***clones_IST*** (the number of all PSU clones over all analyzed fields-of-view for **(a)** or the number of IST clones in all analyzed PSUs for **(b)**).

- **(a)** ***c_PSU*** or **(b)** ***c_IST*** (the number of B, G, Y, R clones among all PSU clones for **(a)** or the number of B, G, Y, R clones among all IST clones for **(b)**).

- **(a)** ***n_replicates_IFE*** or **(b)** ***n_replicates_SG*** (number of times an IFE clone was detected and compared to the surrounding PSUs in the empirical data for **(a)** or the number of times an SG clone was detected and correlated to the adjacent isthmus in the empirical data for **(b)**; corresponds to the number of replicates in each mouse).

We then randomly sampled with replacement from the specified empirical data using the following approach:

1. Sample once from ***clones_per_IFE*** or ***clones_per_SG*** to get an IFE clone number ***n_IFE*** for **(a)** or an SG clone number ***n_SG*** for **(b)**.

2. Sample ***n_IFE***-times from ***c_IFE*** or ***n_SG***-times from ***c_SG*** to assign a color to each IFE clone for **(a)** or each SG clone for **(b)**.

3. Sample once from ***clones_per_PSU*** or ***clones_per_IST*** to get a PSU clone number ***n_PSU*** for **(a)** or an IST clone number ***n_IST*** for **(b)**.

4. Sample ***n_PSU***-times from ***c_PSU*** or ***n_IST***-times from ***c_IST*** to assign a color to each PSU clone for **(a)** or each IST clone for **(b)**.

5. Compare each randomly colored IFE clone to each of the respective PSU clones for **(a)** or each randomly colored SG clone to each clone in the respective IST **(b)**. Count a **correlation** event if at least one PSU clone **(a)** / IST clone **(b)** has the same color as the IFE clone **(a)** / SG clone **(b)**. Count a **non-correlation** event if no PSU clone **(a)** / IST clone **(b)** has the same color as the IFE clone **(a)** / SG clone **(b)**. Count an **alone** event if the number of PSU **(a)** / IST **(b)** clones is equal to 0.

6. Repeat steps 1 – 5 ***n_replicates_IFE***-times for **(a)** or ***n_replicates_SG***-times for **(b)** that equals the number of replicates of the empirical data analysis for each mouse. Return the relative values for **correlation**, **non-correlation** and **alone** events.

7. Repeat steps 1 – 6 **1000**-times to yield a distribution of relative values of **correlation**, **non-correlation** and **alone** events which reflects the expected null distribution if there is no exchange between compartments.

SUPPLEMENTAL REFERENCE

Driskell, R.R., Giangreco, A., Jensen, K.B., Mulder, K.W., and Watt, F.M. (2009). Sox2-positive dermal papilla cells specify hair follicle type in mammalian epidermis. Development *136*, 2815-2823.